

Solvation Structure of Lithium Bromide in Concentrated Acetone Solutions

Yasuo Kameda,* Naomi Kudoh, Shun Suzuki, Takeshi Usuki, and Osamu Uemura

Department of Material and Biological Chemistry, Faculty of Science, Yamagata University, Yamagata 990-8560

(Received October 24, 2000)

Polarized Raman scattering and neutron diffraction measurements have been carried out for concentrated LiBr acetone solutions, in order to deduce detailed information on the solvation structure of Li^+ in non-aqueous solutions. Isotropic Raman spectra observed for $(LiBr)_x[(CH_3)_2C{=}O]_{1-x}$ with $x = 0.02$–0.06 exhibited a polarized peak at $\nu \approx 370$ cm^{-1} which is attributable to the interionic vibration of $Li^+\cdots Br^-$ ion pair which is formed in the solutions. The neutron distribution function around Li^+, $G_{Li}(r)$, derived from the first-order difference function between $^6Li/^7Li$ isotopically substituted 6 mol% LiBr acetone-d_6 solutions indicated the presence of a well-defined first solvation shell around Li^+ in the solution. The nearest neighbor $Li^+\cdots O$(acetone) distance, r_{LiO}, and coordination number, n_{LiO}, were respectively determined to be 2.24(1) Å and 3.2(1), from the least squares fitting analysis for the observed difference interference function, $\Delta_{Li}(Q)$. Structure parameters for the nearest neighbor $Li^+\cdots Br^-$ interaction were determined to be $r_{LiBr} = 2.86(2)$ Å and $n_{LiBr} = 0.8(1)$, respectively.

The elucidation of the solvation structure around the alkali metal ion in organic solvents is indispensable for understanding the reaction mechanism of various organometallic compounds (e.g. synthetic reaction of CH_3Li[1] and C_2H_5Li[2] in ether). Lithium halogenides are considered to be one of the most suitable solutes for probing the microscopic structural information concerning the ion-solvent interactions, as well as the ion-ion interactions because of their high solubilities in various organic solvents. Although the hydration structure of Li^+ in aqueous lithium halogenide solutions has been extensively investigated by means of X-ray[3–16] and neutron diffraction[17–32] techniques, only a limited number of structural studies on solvated Li^+ in organic lithium halogenide solutions have been reported.

The neutron diffraction study on $^6Li/^7Li$ isotopically substituted 0.58M LiBr acetonitrile solutions by Cartailler et al.[21] has revealed that Li^+ is surrounded by, on the average, three acetonitrile molecules and ca. one bromide ion ($r_{LiBr} = 2.46$ Å), and that the nitrogen atom contained in each of the three CD_3CN molecules faces towards Li^+ ($r_{LiN} = 2.05$ Å). More recently, the present authors' group has investigated the solvation structure of Li^+ in highly concentrated methanolic LiBr and LiI solutions by use of the neutron diffraction with the $^6Li/^7Li$ isotopic substitution method.[32,33] We reported that the $Li^+\cdots O$(methanol) interatomic distance, r_{LiO}, and the coordination number, n_{LiO}, are 1.97(6) Å and 3.0(5) for the 25 mol% LiBr solution, and $r_{LiO} = 1.93(6)$ Å and $n_{LiO} = 1.8(5)$ for the 33 mol% LiI one, respectively. In addition, the low-frequency isotropic Raman spectra observed for the concentrated methanolic LiBr solution[32] has been evidence for the formation of a contact ion pair $Li^+\cdots Br^-$. Far-infrared absorption spectra for various organic solutions containing alkali metal ions have been studied by Popov et al.[34–39] and by French and Wood.[40] Absorption bands characteristic for each kind of alkali metal ion have been found out, for example, at $\nu = 400$–430 cm^{-1} for Li^+, 170–200 cm^{-1} for Na^+, and 140–150 cm^{-1} for K^+, respectively. These absorption bands have been assigned to the intermolecular vibration between the cation and solvent molecules. It may be of considerable interest to investigate structural details of the interaction between the carbonyl oxygen atom of the organic solvent molecule and Li^+, which have not yet been obtained. Neutron diffraction with $^6Li/^7Li$ isotopic substitution method is considered to be one of the most suitable experimental techniques to deduce the solvation structure around Li^+ in the solution.

In this paper, we report results of low-frequency isotropic Raman scattering and neutron diffraction measurements for concentrated LiBr acetone solutions, in order to deduce detailed structural information concerning the first solvation shell around Li^+ as well as to investigate the formation of the $Li^+\cdots Br^-$ pair in lithium halogenide acetone solutions.

Experimental

Materials. ^6Li-enriched lithium bromide was prepared by reacting $^6Li_2CO_3$ (95.45% ^6Li, Tomiyama Chemical Co., Ltd.) with a slight excess of the concentrated aqueous hydrobromic acid solution (Nacalai Tesque, Guaranteed grade). The product solution was dehydrated by heating at 180 °C under vacuum. Anhydrous $^{nat}LiBr$ (92.5% ^7Li, natural abundance) was obtained by the dehydration of $^{nat}LiBr{\bullet}H_2O$ (Nacalai Tesque, Guaranteed grade) at 180 °C under vacuum.

Required amounts of anhydrous $^{nat}LiBr$ and ^6LiBr were dissolved into $(CH_3)_2C{=}O$ (natural abundance, Nacalai Tesque, Guaranteed grade), which was dried with molecular sieves 4A (Nacalai Tesque), to prepare 2,4, and 6 mol% LiBr–acetone solutions. The sample solution was sealed into a Pyrex® cell (10 × 10 mm and 40 mmH) and used for the Raman scattering measurement.

Table 1. Isotopic Compositions, Mean Scattering Length, b_{Li}, for Lithium Atom, Total Cross Sections, and the Number Density Scaled in the Stoichiometric Unit $(LiBr)_x[(CD_3)_2C{=}O]_{1-x}$, σ_t, and ρ, Respectively, for Sample Solutions Used in This Study

Samples	^{6}Li/%	^{7}Li/%	$b_{Li}/10^{-12}$ cm[a)]	σ_t/barns[b)]	ρ/Å^{-3}
$(^6LiBr)_{0.06}[(CD_3)_2C{=}O]_{0.94}$	95.5	4.5	0.181	72.162	0.00860
$(^{nat}LiBr)_{0.06}[(CD_3)_2C{=}O]_{0.94}$[c)]	7.5	92.5	−0.190	42.152	

a) Taken from Ref. 41. b) For incident neutron wavelength of 1.090 Å. c) The superscript "nat" denotes the natural abundance.

Weighed amounts of enriched anhydrous *LiBr were dissolved into acetone-d_6 (99.9% D, ISOTEC Inc.) to prepare 6 mol% *LiBr acetone-d_6 solutions with different ^{6}Li/^{7}Li isotopic compositions. Each sample solution was sealed into a cylindrical quartz cell (11.8 mm in inner diameter and 1.1 mm in thickness, respectively) and used for the neutron diffraction measurement. Sample parameters are listed in Table 1. The coherent scattering length, b, and scattering and absorption cross sections, σ_s and σ_a, for the constituent nuclei, were respectively referred to the corresponding ones tabulated by Sears.[41] Scattering cross sections for the deuterium atom within an acetone molecule were employed as values for the "free" scattering cross section, such values were successfully adopted in the data correction for neutron scattering intensities from $NiCl_2$ solutions in deuterated methanol.[42]

Raman Scattering Measurements. The polarized Raman spectrum was obtained at 25 °C in the frequency range of $30 \leq \nu \leq 1200$ cm^{-1} using a JASCO NR-1100 spectrometer with a 514.5 nm line of an NEC GLG-3200 Ar^+ laser operated at 200 mW. The calibration of the monochromator was made using 89 neon emission lines. The efficiency of the polarization filter was carefully checked through the measurement of the depolarization ratio of ν_1, ν_2, and ν_4 vibrational bands of CCl_4 molecule in the liquid state. Details concerning the present Raman scattering measurement are identical to those described in our previous papers.[43,44]

Neutron Diffraction Measurements. Neutron diffraction measurements were carried out at 25 °C using an ISSP 4G (GPTAS) diffractometer installed at the JRR-3M research reactor operated at 20 MW in Japan Atomic Energy Research Institute (JAERI), Tokai, Japan. The incident neutron wavelength, λ = 1.090 ± 0.002 Å, was determined by Bragg reflections from Al powder. Collimations used were 40′−40′−40′ in going from the reactor to detector. The aperture of the collimated beam was 14 mm in width and 32 mm in height. Scattered neutrons from the sample were collected over the angular range of $3 \leq 2\theta \leq 114°$, which corresponds to $0.30 \leq Q \leq 9.67$ Å^{-1} (the scattering vector magnitude, $Q = 4\pi\sin\theta/\lambda$). The step interval was chosen to be $\Delta(2\theta) = 0.5°$ in the range of $3 \leq 2\theta \leq 40°$ and $\Delta(2\theta) = 1°$ in the range of $41 \leq 2\theta \leq 114°$, respectively. The preset neutron monitor counts were 1.80×10^9 and 1.45×10^9 for ^{6}LiBr and ^{nat}LiBr solutions, respectively. Scattering intensities were measured in advance for a vanadium rod (10 mm in diameter), empty cell and background, respectively.

Data Reduction

Raman Scattering Data. The correction of the Bose–Einstein factor for the observed Raman spectrum, which is needed to distinguish low-frequency vibrational components, was made using the equation below:[45–48]

$$I^{corrected}(\nu) = (\nu_0 - \nu)^{-4}\,\nu[1 - \exp(-h\nu/kT)]I^{obs}(\nu), \quad (1)$$

where, ν and ν_0 are the Stokes–Raman shift and frequency of the incident light, respectively. T corresponds to the absolute temperature. The isotropic Raman intensity, $I^{iso}(\nu)$, can be given by

$$I^{iso}(\nu) = I^{//}(\nu) - (4/3)I^{\perp}(\nu), \quad (2)$$

where, $I^{//}(\nu)$ and $I^{\perp}(\nu)$ denote the corrected parallel and perpendicular spectra, respectively. The peak analysis of the isotropic spectrum was performed with a SALS program,[49] assuming a Gaussian peak shape function.

Neutron Diffraction Data. Observed scattering intensities from the sample were corrected for the instrumental background, and absorption,[50] multiple[51] and incoherent scatterings. The observed count rate was then converted to an absolute scale by using scattering intensities from the vanadium rod. The first-order difference function,[52–54] $\Delta_{Li}(Q)$, was determined by taking the numerical difference in the normalized scattering cross section between samples with different Li isotopic compositions. The inelasticity effect, mainly arising from the self scattering contribution by D atom within the acetone molecule, can be expected to disappear through the subtraction of the two scattering cross sections in which the inelasticity distortion is equally involved.

$\Delta_{Li}(Q)$, scaled by the stoichiometric unit, $(LiBr)_x[(CD_3)_2C{=}O]_{1-x}$, can be represented as a linear combination of partial structure factors concerning the Li atom as follows:

$$\begin{aligned}\Delta_{Li}(Q) = {} & A[a_{LiO}(Q) - 1] + B[a_{LiD}(Q) - 1] \\ & + C[a_{LiC}(Q) - 1] + D[a_{LiBr}(Q) - 1] \\ & + E[a_{LiLi}(Q) - 1] + \text{correction term}, \end{aligned} \quad (3)$$

and

$$\begin{aligned} & A = 2x(1-x)(b_{Li} - b'_{Li})b_O,\ B = 12x(1-x)(b_{Li} - b'_{Li})b_D, \\ & C = 6x(1-x)(b_{Li} - b'_{Li})b_C,\ D = 2x^2(b_{Li} - b'_{Li})b_{Br}, \\ & E = x^2({b_{Li}}^2 - {b'_{Li}}^2), \end{aligned}$$

where b_i stands for the mean scattering length of nucleus i. Contributions from atom pairs that do not include Li^+ are canceled out in $\Delta_{Li}(Q)$. The correction term in Eq. 3 arises by a slight difference in the inelasticity contribution in the self scattering term between ^{6}Li and ^{7}Li, which is expected to be negligibly small. Coefficients of respective partial structure factors in $\Delta_{Li}(Q)$ are listed in Table 2.

The Fourier transform of $\Delta_{Li}(Q)$ corresponds to the distribution function around Li^+, $G_{Li}(r)$,

Table 2. Values of the Coefficients of $a_{ij}(Q)$ in Eq. 3

A/barns	B/barns	C/barns	D/barns	E/barns
0.02431	0.16742	0.08351	0.00182	−0.00001

$$G_{Li}(r) = 1 + (2\pi^2\rho r)^{-1}(A+B+C+D+E)^{-1}\int_0^{Q_{max}} Q\Delta_{Li}(Q)\sin(Qr)dQ$$
$$= [Ag_{LiO}(r) + Bg_{LiD}(r) + Cg_{LiC}(r) + Dg_{LiBr}(r) + Eg_{LiLi}(r)]\times (A + B + C + D + E)^{-1}, \quad (4)$$

where ρ is the number density of atoms scaled in the stoichiometric unit $(LiBr)_x[(CD_3)_2C{=}O]_{1-x}$. $g_{Lij}(r)$ denotes the partial distribution function for Li–j atom pair. The upper limit, Q_{max}, in the Fourier integral was taken to be 9.67 Å^{-1} in the present work. The self-consistency of the observed $\Delta_{Li}(Q)$ was carefully checked by the following procedures. i) The observed $\Delta^0_{Li}(Q)$ was firstly Fourier transformed to obtain $G^0_{Li}(r)$. ii) Unphysical features which appeared in the $G^0_{Li}(r)$ at the subatomic region below $r = 1.2$ Å was then removed. iii) Corrected $G^0_{Li}(r)$ was back-transformed to obtain $\Delta^1_{Li}(Q)$ in which low-frequency systematic errors due to slight imbalance of the H atom and small uncertainties in the absorption correction were eliminated. iv) The difference between $\Delta^0_{Li}(Q)$ and $\Delta^1_{Li}(Q)$ was extensively smoothed to obtain the correction function. It was confirmed that the correction function did not exhibit any sudden fluctuation. v) The correction function was subtracted from the observed $\Delta^0_{Li}(Q)$ to obtain fully corrected $\Delta_{Li}(Q)$, and employed in the subsequent least squares analysis.

Structural parameters concerning the first coordination shell of Li^+ in the solution were determined by the least squares refinement analysis of the observed $\Delta_{Li}(Q)$. The theoretical interference function, $\Delta_{Li}^{calc}(Q)$, is written as the sum of short- and long-range interactions as the following equation:[55–57]

$$\Delta_{Li}^{calc}(Q) = \Sigma\, 2xn_{Lij}(b_{Li} - b'_{Li})b_j\exp(-l_{Lij}^2Q^2/2) \times \sin(Qr_{Lij})/(Qr_{Lij}) + 4\pi\rho\,(A + B + C + D + E) \times \exp(-l_{0Lij}^2Q^2/2)[Qr_{0Lij}\cos(Qr_{0Lij}) - \sin(Qr_{0Lij})]]Q^{-3}, \quad (5)$$

where n_{Lij}, l_{Lij} and r_{Lij} denote the coordination number, root mean square amplitude, and interatomic distance for Li–j pair, respectively. The long-range parameter, r_{0Lij}, is the distance beyond which the uniform distribution of j atoms around Li^+ is assumed, and l_{0Lij} describes the sharpness of the boundary at r_{0Lij}. The theoretical $\Delta_{Li}^{calc}(Q)$ was evaluated on the basis of the following assumptions. a) For the interaction between Li^+ and the nearest neighbor acetone molecule, structural parameters, r_{LiO}, l_{LiO}, n_{LiO}, the bond angle, α (= $\angle Li^+\cdots O{=}C_1$), and the dihedral angle β between the molecular plane of the acetone molecule, and the plane involving Li^+, O, and C_1 atoms, were treated as independent parameters. The molecular geometry of the acetone molecule is fixed to those observed in gaseous[58–64] and liquid[65,66] states. The r.m.s. amplitudes for non-bonding interaction within the nearest neighbor $Li^+\cdots$acetone unit, l_{Lij}, were approximated through the following equation:[55]

$$l_{Lij} = l_{LiO} \times (r_{Lij}/r_{LiO})^{1/2} \quad (6)$$

where r_{Lij} denotes the calculated intermolecular distance within the structural unit. b) It was suggested in the preliminary analysis of $\Delta_{Li}(Q)$ that a significant improvement of the fit is feasible by introducing the contribution from $Li^+\cdots Br^-$ ion pair located at $r \approx 2.8$ Å. We therefore involved the nearest neighbor $Li^+\cdots Br^-$ contribution to the theoretical $\Delta_{Li}^{calc}(Q)$. Parameters, r_{LiBr}, l_{LiBr}, and n_{LiBr}, were allowed to vary independently. c) The contribution from acetone molecules within the second solvation shell around Li^+ was also introduced to improve the fit in the low-Q region. They were treated as a single interaction, in which the sum of coherent scattering lengths of constituent atoms within a single acetone molecule; $6b_D + 3b_C + b_O$, was taken as the coherent scattering length b_j in Eq. 5. d) Structural parameters for the continuous long-range distribution of atoms, such as l_{0Lij} and r_{0Lij}, were taken to be identical for all $Li^+\cdots$j (j = C, O, D, Br, and Li) interactions for the sake of reducing the number of independent parameters. The least squares refinement was carried out in the range of $0.3 \le Q \le 9.6$ Å^{-1} using a SALS program,[49] assuming statistical errors distribute uniformly.

Results and Discussion

Low-Frequency Isotropic Raman Spectra. The composition dependence of observed low-frequency isotropic Raman spectra for LiBr–acetone solutions is shown in Fig. 1. The intensity of polarized peaks centered at $\nu \approx 100$ and ≈ 370 cm^{-1} exhibit a systematic increase with increasing LiBr content. Since there is no indication of polarized peaks in this ν region in the spectrum for pure liquid acetone, these polarized peaks obviously reflect the effect of solute–solvent or solute–solute interactions. Results of the least squares fitting analysis applied to the observed spectra, using two Gaussian peaks with the background function which can be approximated by the third polynomial function of ν, are summarized in Table 3.

The position of the peak B for ^{nat}LiBr solutions falls at almost the same ν value of 365–370 cm^{-1}, irrespective of LiBr

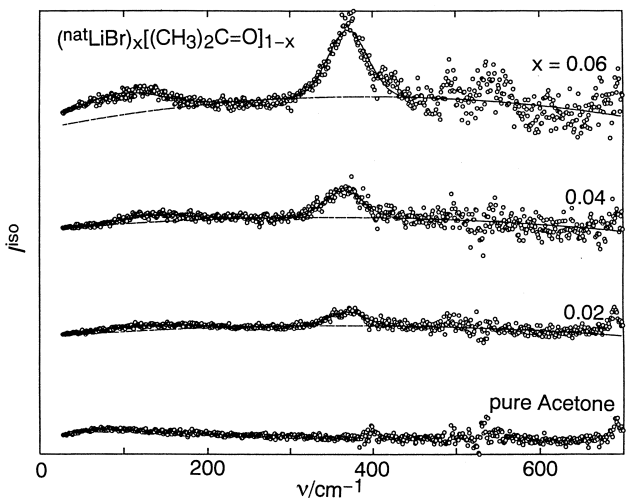

Fig. 1. Composition dependence of the isotropic Raman spectrum for LiBr–acetone solutions, $(LiBr)_x[(CH_3)_2{-}C{=}O]_{1-x}$, at 25 °C. The Gaussian components derived from a least squares fit are indicated by solid lines.

Table 3. The Peak Position, Full Width at Half Maximum, and Peak Height of Gaussian Components Derived from the Least Squares Fit of the Isotropic Raman Spectra for LiBr–Acetone Solutions, ν, w, and h, Respectively[a)]

		Peak A			Peak B		
x	Solute	ν/cm^{-1}	w/cm^{-1}	h	ν/cm^{-1}	w/cm^{-1}	h
0.06	^{nat}LiBr	93(2)	122(7)	0.31(1)	370.3(5)	55(1)	0.96(1)
0.06	^{6}LiBr	115(4)	131(12)	0.18(1)	395.6(9)	79(2)	0.59(1)
0.04	^{nat}LiBr	138(4)	95(9)	0.102(9)	365.3(8)	54(1)	0.39(1)
0.02	^{nat}LiBr	127(3)	127(13)	0.076(6)	369.2(7)	49(1)	0.202(6)

a) Estimated standard deviations are given in parentheses.

content. The position of the peak B for the ^{6}LiBr solution shifts to ca. 25 cm^{-1} higher frequency side, implying that Li^+ should move during the intermolecular vibration. The present position of the peak B is in good agreement with the frequency of the $Li^+\cdots Br^-$ stretching vibrational mode observed in highly concentrated 20 and 25 mol% LiBr methanolic solutions, in which the formation of contact ion pair, $Li^+\cdots Br^-$, is suggested.[32] The isotopic shift for this peak in the methanolic solution has been reported to be 22 cm^{-1}, which is very close to the present value for the acetone solution. The $Li^+\cdots Br^-$ interionic vibrational band has also been obtained as the polarized Raman peak centered at $\nu \approx 340$ cm^{-1} in highly concentrated aqueous LiBr solutions,[43,67] in which the formation of contact ion pair is confirmed by our previous neutron diffraction study.[30] Consequently, the Raman peak B observed for the present acetone solutions can be reasonably attributed to the $Li^+\cdots Br^-$ interionic vibration. Since the peak B can clearly be observed even for the spectrum for 2 mol% LiBr concentration, the formation of $Li^+\cdots Br^-$ contact ion pair seems to occur at considerably lower solute concentrations in the acetone solution. This may be compared with cases of methanolic LiBr[32] and aqueous LiBr[43,67] solutions, in which the $Li^+\cdots Br^-$ vibrational band appears only at higher solute concentrations above ca. 20 mol% LiBr.

The assignment of the peak A is less clear at present, because of the strong Rayleigh background at the lower-frequency limit in observed parallel and perpendicular spectra. The Li+$\cdots$methanol intermolecular vibrational mode has been observed at $\nu \approx 150$ cm^{-1} as the polarized peak in the isotropic Raman spectrum for highly concentrated methanolic LiBr solutions.[32] The Raman peak A observed for the present acetone solutions might be attributable to the $Li^+\cdots$acetone intermolecular vibrational mode.

Neutron Diffraction. The difference function, $\Delta_{Li}(Q)$, observed for 6 mol% LiBr–acetone solution is shown in Fig. 2a. Diffraction peaks located at $Q \approx 1.7$ and 3 Å^{-1} are obviously identified, as well as a small pre-peak at $Q \approx 0.8$ Å^{-1}. The oscillational feature of $\Delta_{Li}(Q)$ extends to the higher-Q region. The observed distribution function around Li^+, $G_{Li}(r)$, is represented in Fig. 3. A dominant first peak at $r \approx 2.2$ Å and the second peak appearing at $r \approx 4.3$ Å in the present $G_{Li}(r)$, clearly indicate the existence of well-defined first solvation shell around Li^+ in this solution. The first peak at $r \approx 2.2$ Å is attributable to the nearest neighbor $Li^+\cdots$O(acetone) interaction from the electrostatic point of view. If we assume this first peak as the $Li^+\cdots$O interaction, the number of oxygen atom around Li^+ can be estimated to be ca. 3 from the integration of the present $G_{Li}(r)$ in the range of $1.6 \le r \le 2.6$ Å. The second

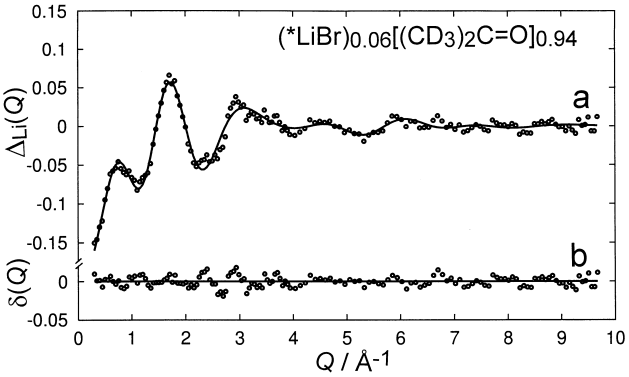

Fig. 2. a) Difference function, $\Delta_{Li}(Q)$, observed for 6 mol% LiBr–acetone solution (circles). The best-fit of calculated interference terms in Eq. 5 (solid line). b) The residual function, $\delta(Q)$ (circles).

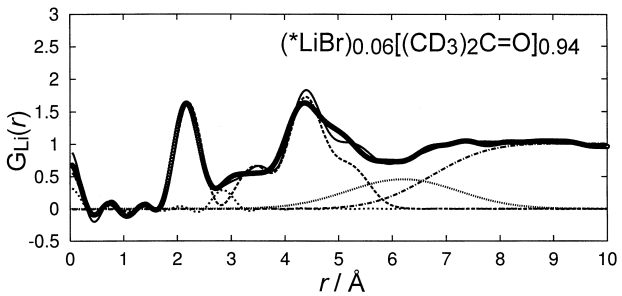

Fig. 3. Distribution function around Li^+, $G_{Li}(r)$, observed for 6 mol% LiBr–acetone solution (circles). The Fourier transform of the line in Fig. 2a (solid line). Contributions from short-range $Li^+\cdots$acetone(I), $Li^+\cdots Br^-$, and $Li^+\cdots$acetone(II) are denoted by broken-, thick dotted-, and thin dotted lines, respectively. A dashed-dot line indicates the long-range interaction.

peak located at $r \approx 4.3$ Å is considered to involve interactions between Li^+ and carbon and deuterium atoms within the acetone molecule in the first solvation shell. In the crystalline LiBr–acetone complex, LiBr•$(CH_3)_2C{=}O$, Li^+ is coordinated with two oxygen atoms of two acetone molecules (r_{LiO} = 1.9(1) and 2.0(1) Å) and with two bromide ions (r_{LiBr} = 2.55(2) and 2.51(2) Å).[68] Lithium and bromide ions are found to form a four-membered Li_2Br_2 ring in this crystalline compound.[68] The nearest neighbor short-range structure around Li^+ in concentrated LiBr–acetone solution may be considerably different from that reported in the crystalline complex.

Table 4. Results of the Least-Squares Refinement for the Observed $\Delta_{Li}(Q)$[a)]

$i\cdots j$	r_{ij}/Å	l_{ij}/Å	n_{ij}	α/° [b)]	β/° [c)]
$Li^+\cdots O$(acetone I)[d)]	2.24(1)	0.21(1)	3.2(1)	171(1)	20(2)
$Li^+\cdots Br^-$	2.86(2)	0.10(5)	0.8(1)		
$Li^+\cdots X$(acetone II)e)	6.37(1)	1.01(1)	4.8(2)		
	r_{0ij}/Å	l_{0ij}/Å			
Long-range	5.55(1)	0.84(1)			

a)Estimated standard deviations are given in parentheses. b) Bond angle $\angle Li^+\cdots O{=}C_1$. c) Dihedral angle between the molecular plane of acetone and the plane involving Li^+, O, and C_1 atoms. d) The first nearest neighbor $Li^+\cdots$acetone interaction. e) The second nearest neighbor $Li^+\cdots$acetone interaction, which is treated as a single interaction in the present analysis.

We next carried out the least squares fitting analysis of the observed $\Delta_{Li}(Q)$ to determine structural parameters concerning the first solvation shell around Li^+; the result of this fit is indicated in Fig. 2. A satisfactory agreement is obtained between observed and calculated $\Delta_{Li}(Q)$ in the whole Q-range. Final values of all independent parameters are summarized in Table 4. The nearest neighbor $Li^+\cdots O$ distance, r_{LiO}, and coordination number, n_{LiO}, are determined to be 2.24(1) Å and 3.2(1), respectively. The bond angle α (= $Li^+\cdots O{=}C_1$) and the dihedral angle β between the molecular plane of acetone molecule and a plane involving Li^+, O, and C_1 atoms, were obtained to be 171(1)° and 20(2)°, respectively. A slight departure of the present bond angle, α, from the linear $Li^+\cdots O{=}C_1$ coordination, which has been predicted for isolated $Li^+\cdots$formaldehyde complex from the molecular orbital calculation,[69] may be interpreted by the packing effect which may occur in the acetone solution. The present $Li^+\cdots O$ distance is ca. 0.2 Å longer than that observed in concentrated aqueous[17–32] and methanolic[33,34] lithium halogenide solutions, in which hydroxyl oxygen atoms are strongly coordinated to the Li^+ characterized by the presence of well resolved $Li^+\cdots O$ stretching vibrational bands observed in the isotropic Raman spectra.[32,43] On the other hand, less definitive interaction of the $Li^+\cdots O$(acetone) peak has been obtained in the present isotropic Raman spectra, which is consistent with the result from the neutron data. Present results are therefore considered to represent a significant difference in the $Li^+\cdots O$ interaction between solvents involving the hydroxyl- and the carbonyl oxygen atoms in solution. The present value of the nearest neighbor $Li^+\cdots Br^-$ distance, r_{LiBr} = 2.86(2) Å, is in good agreement with that observed in crystalline lithium bromide monohydrates (r_{LiBr} = 2.85 Å, for β-LiBr•H_2O and r_{LiBr} = 2.84 Å, for α-LiBr•H_2O).[70] The coordination number, n_{LiBr}, is determined to be 0.8(1), implying that the contact ion pair, $Li^+\cdots Br^-$, is formed in the present solution. The result is consistent with that obtained from the present isotropic Raman spectra as described in the previous section. In the present solution, Li^+ is surrounded by, on the average, ca. one Br^- and ca. three acetone molecules, with each oxygen atom of the acetone molecule facing toward central Li^+. It has also been revealed that ca. five acetone molecules are involved in the second solvation shell of Li^+ with a much broadened distribution centered at 6.37 Å, which cannot be decomposed at the present time. To obtain unambiguous information on the configuration of acetone molecules in the second solvation shell, it is necessary to determine partial distribution functions such as $g_{LiO}(r)$, $g_{LiC}(r)$, and $g_{LiH}(r)$, which are given through further experiment including H/D isotopic substitutions. Along this line, data analyses of H/D isotopically substituted solutions are now in progress.

The authors would like to express their thanks to The Institute of Solid State Physics (ISSP), University of Tokyo, for allowing us to use the 4G diffractometer in JRR-3M. We are also grateful to Professor Hideki Yoshizawa (University of Tokyo) and Mr. Yoshihisa Kawamura (University of Tokyo) for their help during the course of the neutron diffraction measurement. All of the calculations were carried out with the S7/7000U computer at the Yamagata University Computing Service Center. This work was partially supported by a Grant-in-Aid for Scientific Research No. 12640534 from the Ministry of Education, Science, Sports, and Culture.

References

1 G. Wittig and A. Hasse, *Org. Synth.*, **50**, 67 (1970).
2 H. Gilman, F. W. Moor, O. Baire, *J. Am. Chem. Soc.*, **63**, 2480 (1941).
3 G. W. Brady, *J. Chem. Phys.*, **28**, 464 (1958).
4 R. M. Lawrence and R. F. Kruh, *J. Chem. Phys.*, **47**, 4758 (1967).
5 G. Licheri, G. Piccaluga, and G. Pinna, *J. Appl. Crystallogr.*, **6**, 392 (1973).
6 A. H. Narten, F. Vaslow, and H. A. Levy, *J. Chem. Phys.*, **58**, 5017 (1973).
7 G. Licheri, G. Piccaluga, and G. Pinna, *Chem. Phys. Lett.*, **35**, 119 (1975).
8 G. Pálinkás, T. Radnai, and F. Hajdu, *Z. Naturforsch.*, **35a**, 107 (1980).
9 T. Radnai, G. Pálinkás, Gy. I. Szász, and K. Heinzinger, *Z. Naturforsch.*, **36a**, 1076 (1981).
10 P. Bopp, I. Okada, H. Ohtaki, and K. Heinzinger, *Z. Naturforsch.*, **40a**, 116 (1985).
11 K. Tanaka, N. Ogita, Y. Tamura, I. Okada, H. Ohtaki, G. Pálinkás, E. Spohr, and K. Heinzinger, *Z. Naturforsch.*, **42a**, 29 (1987).
12 Y. Tamura, T. Yamaguchi, I. Okada, and H. Ohtaki, *Z. Naturforsch.*, **42a**, 367 (1988).
13 Y. Tamura, K. Tanaka, E. Spohr, and K. Heinzinger, *Z. Naturforsch.*, **43a**, 1103, (1988).
14 K. Yamanaka, M. Yamagami, T. Takamuku, T. Yamaguchi, and H. Wakita, *J. Phys. Chem.*, **97**, 10835 (1993).
15 T. Yamaguchi, M. Yamagami, H. Wakita, and A. K. Soper,

J. Mol. Liq., **65/66**, 91 (1995).
16 T. Takamuku, M. Yamagami, H. Wakita, and T. Yamaguchi, *Z. Naturforsch.*, **52a**, 521 (1997).
17 N. Ohtomo and K. Arakawa, *Bull. Chem. Soc. Jpn.*, **52**, 2755 (1979).
18 J. R. Newsome, G. W. Neilson, and J. E. Enderby, *J. Phys. C: Solid State Phys.*, **13**, L923 (1980).
19 K. Ichikawa, Y. Kameda, T. Matsumoto, and M. Misawa, *J. Phys. C: Solid State Phys.*, **17**, L725 (1984).
20 K. Ichikawa and Y. Kameda, *J. Phys. Condens. Matter*, **1**, 257 (1989).
21 T. Cartailler, W. Kuntz, P. Turq, and M-C. Bellisent-Funel, *J. Phys.: Condens. Matter*, **3**, 9511 (1991).
22 K. Ichikawa, S. Kotani, M. Izumi, and T. Yamanaka, *Mol. Phys.*, **77**, 677 (1992).
23 R. H. Tromp, G. W. Neilson, and A. K. Soper, *J. Chem. Phys.*, **96**, 8460 (1992).
24 Y. Kameda and O. Uemura, *Bull. Chem. Soc. Jpn.*, **66**, 384 (1993).
25 M. Yamagami, T. Yamaguchi, H. Wakita, and M. Misawa, *J. Chem. Phys.*, **100**, 3122 (1994).
26 B. Prével, J. F. Jal, J. Dupuy-Philon, and A. K. Soper, *J. Chem. Phys.*, **103**, 1886 (1995).
27 B. Prével, J. F. Jal, J. Dupuy-Philon, and A. K. Soper, *J. Chem. Phys.*, **103**, 1897 (1995).
28 T. Yamaguchi, M. Yamagami, H. Ohzono, K. Yamanaka, and H. Wakita, *Physica B*, **213&214**, 480 (1995).
29 I. Howell and G. W. Neilson, *J. Phys.: Condens. Matter*, **8**, 4455 (1996).
30 Y. Kameda, S. Suzuki, H. Ebata, T. Usuki, and O. Uemura, *Bull. Chem. Soc. Jpn.*, **70**, 47 (1997).
31 S. Ansell, J. Dupuy-Philon, J. F. Jal, and G. W. Neilson, *J. Phys.: Condens. Matter*, **9**, 8835 (1997).
32 Y. Kameda, T. Usuki, and O. Uemura, *High Temperature Materials and Processes*, **18**, 27 (1999).
33 Y. Kameda, H. Ebata, T. Usuki, and O. Uemura, *Physica B*, **213&214**, 477 (1995).
34 B. W. Maxey and A. I. Popov, *J. Am. Chem. Soc.*, **89**, 2230 (1967).
35 B. W. Maxey and A. I. Popov, *J. Am. Chem. Soc.*, **91**, 20 (1969).
36 J. L. Wuepper and A. I. Popov, *J. Am. Chem. Soc.*, **91**, 4352 (1969).
37 W. J. McKinney and A. I. Popov, *J. Phys. Chem.*, **74**, 535 (1970).
38 J. L. Wuepper and A. I. Popov, *J. Am. Chem. Soc.*, **92**, 1493 (1970).
39 M. K. Wong, W. J. McKinney, and A. I. Popov, *J. Phys. Chem.*, **75**, 56 (1971).
40 M. J. French and J. L. Wood, *J. Chem. Phys.*, **49**, 2358 (1968).
41 V. F. Sears, "Thermal-Neutron Scattering Lengths and Cross Sections for Condensed Matter Research," AECL-8490, Atomic Energy of Canada Ltd., (1984), p. 16.
42 D. H. Powell and G. W. Neilson, *J. Phys.: Condens. Matter*, **2**, 5867 (1990).
43 Y. Kameda, H. Ebata, and O. Uemura, *Bull. Chem. Soc. Jpn.*, **67**, 929 (1994).
44 Y. Kameda, I. Sugawara, K. Kijima, T. Usuki, and O. Uemura, *Bull. Chem. Soc. Jpn.*, **68**, 512 (1995).
45 G. W. Chantry, "The Raman Effect," ed by A. Anderson, Marcel Dekker Inc., New York (1971) Vol. 1, p. 70.
46 J. R. Scherer, M. K. Go, and S. Kint, *J. Phys. Chem.*, **78**, 1034 (1974).
47 M. Lucas, A. De Trobriand, and M. Ceccaldi, *J. Phys. Chem.*, **79**, 913 (1975).
48 M. Moskovits and K. H. Michalian, *J. Chem. Phys.*, **69**, 2306 (1978).
49 T. Nakagawa and Y. Oyanagi, "Recent Developments in Statistical Inference and Data Analysis," ed by K. Matushita, North-Holland (1980), p. 221.
50 H. H. Paalman and C. J. Pings, *J. Appl. Phys.*, **33**, 2635 (1962).
51 I. A. Blech and B. L. Averbach, *Phys. Rev.*, **137**, A1113 (1965).
52 A. K. Soper, G. W. Neilson, J. E. Enderby, and R. A. Howe, *J. Phys. C: Solid State Phys.*, **10**, 1794 (1977).
53 G. W. Neilson, R. D. Broadbent, I. Howell, and R. H. Tromp., *J. Chem. Soc., Faraday Trans.*, **89**, 2927 (1993).
54 J. E. Enderby, *Chem. Soc. Rev.*, **24**, 159 (1995).
55 A. H. Narten, M. D. Danford, and H. A. Levy, *Discuss. Faraday Soc.*, **43**, 97 (1967).
56 R. Caminiti, P. Cucca, M. Monduzzi, G. Saba, and G. Crisponi, *J. Chem. Phys.*, **81**, 543 (1984).
57 H. Ohtaki, and N. Fukushima, *J. Solution Chem.*, **21**, 23 (1992).
58 P. W. Allen, H. J. Bowen, L. E. Sutton, and O. Bastiansen, *Trans. Faraday Soc.*, **48**, 991 (1952).
59 C. Romers and J. E. G. Creutzberg, *Rec. Trav. Chim.*, **75**, 331 (1956).
60 J. D. Swalen and C. C. Costain, *J. Chem. Phys.*, **31**, 1562 (1959).
61 C. Kato, S. Konaka, T. Iijima, and M. Kimura, *Bull. Chem. Soc. Jpn.*, **42**, 2148 (1969).
62 T. Iijima, *Bull. Chem. Soc. Jpn.*, **43**, 1049 (1970).
63 R. L. Hiderbrandt, A. L. Andreassen, and S. H. Bauer, *J. Phys. Chem.*, **74**, 1586 (1970).
64 T. Iijima, *Bull. Chem. Soc. Jpn.*, **45**, 3526 (1972).
65 H. Bertagnolli and M. Hoffmann, *Z. Phys. Chem.*, **159**, 185 (1988).
66 H. Bertagnolli, M. Hoffmann, and M. Ostheimer, *Z. Phys. Chem.*, **165**, 165 (1989).
67 W. Rudolph, M. H. Brooker, and C. C. Pye, *J. Phys. Chem.*, **99**, 3793 (1995).
68 R. Amstutz, J. D. Dunitz, T. Laube, W. B. Schweizer, and D. Seebach, *Chem. Ber.*, **119**, 434 (1986).
69 J. E. D. Bene, M. J. Frish, K. Raghavachari, J. A. Pople, and P. von R. Schleyer, *J. Phys. Chem.*, **87**, 73 (1983).
70 E. Weiss, H. Hensel, and H. Kühr, *Chem. Ber.*, **102**, 632 (1969).